Genetic-algorithm retrieval of the molecular alignment distribution with high-order harmonics generated from transiently aligned CO_2 molecules

Changzhi Jiang,[1] Haoran Jiang,[1] Yanbo Chen,[1] Baochang Li,[1] C. D. Lin,[2] and Cheng Jin[1,3,*]

[1]*Department of Applied Physics, Nanjing University of Science and Technology, Nanjing, Jiangsu 210094, China*

[2]*J. R. Macdonald Laboratory, Department of Physics, Kansas State University, Manhattan, Kansas 66506, USA*

[3]*MIIT Key Laboratory of Semiconductor Microstructure and Quantum Sensing, Nanjing University of Science and Technology, Nanjing, Jiangsu 210094, China*

(Received 20 December 2021; accepted 7 February 2022; published 22 February 2022)

Using genetic algorithm, we propose a method to retrieve the alignment distribution of transiently aligned CO_2 molecules from the high-order harmonic generation (HHG) spectra. The retrieval method is based on the quantitative rescattering (QRS) model where averaged photorecombination transition dipole can be factored out from the parallel (or perpendicular) harmonic spectra after the propagation of the harmonic fields in the gas medium. We examine how the retrieved alignment distributions are affected by uncertainty in alignment-dependent ionization probability and on multiple orbital contribution to the HHG. We further confirm that alignment distribution is more accurately retrieved by using the minima in the HHG spectra driven by a long-wavelength laser. In addition, we show that earlier experimental data on the ratios between the perpendicular and the parallel HHG components of aligned CO_2 molecules are in better agreement with the QRS model if the macroscopic propagation and multiple orbital interference are included in the theoretical calculation.

DOI: 10.1103/PhysRevA.105.023111

I. INTRODUCTION

Since the 1990s, the availability of intense short laser pulses makes it possible to align molecules in the gas phase [1,2]. The most popular scheme is to kick molecules impulsively [3–5]. In this scheme, partial alignment occurs periodically in the form of fractional and full revivals long after the aligning laser (also called the pump laser) is over. Experiments with aligned molecules can be performed under the field-free condition. Since fixed-in-space molecules don't have spherical symmetry, the molecules respond to an intense laser field differently depending on their alignment with respect to the laser polarization direction. Thus, it is expected that rich dynamical information in laser-matter interaction can be probed beyond what is available from randomly distributed ones [6,7]. Besides applications in probing chemical reaction dynamics [8], aligned molecules have also been widely employed to study strong-field phenomena, such as high-order harmonic generation (HHG) [9,10], tomographic imaging [11,12], laser-induced electron diffraction [13,14], multiphoton and tunneling ionization [15], etc. For these applications, it is crucial to accurately characterize the alignment distribution (or the alignment degree). For linear molecules, the alignment can be described by the angular distribution function $\rho(\theta)$ [16], where θ is the angle between the molecular axis and the polarization direction of the pump laser. However, it is challenging to precisely measure the intensity of the aligning laser pulse or the gas temperature, both of which are the key parameters for determining the alignment distribution. Although different methods have been proposed or employed to obtain the alignment distribution from the pump pulse, through the angular dependence of strong-field ionization [17], or the Coulomb explosion imaging [18–21], other more accurate approaches for measuring or retrieving the alignment distribution of molecules are desirable. We comment that the method of Coulomb explosion imaging has been widely used previously for determining the alignment distribution by double ionizing the molecules with an intense laser. This method measures the coincident ion momentum vectors after the ions have reached the detector. The method would fail if the molecular axis changes from the gas cell to the detector, or when the molecular axis has rotated in the laser field where postionization alignment effect [22,23] is significant.

HHG from molecules is a well-known ultrafast nonlinear process in which an intense femtosecond laser ionizes a valence electron, accelerates it, and then drives it back to recombine with the parent ion, to emit high-energy photons [24,25]. Combined with laser alignment, the molecular HHG has been applied for understanding molecular structure and electron correlations [26,27] and probing ultrafast dynamics in molecules [28–30], reconstructing the molecular orbital [12,31–33], and so on. Recently, it has been proposed to obtain alignment distribution of molecules by using high harmonics generated when molecules are transiently aligned [34]. For example, in He *et al.* [35], by using the sensitive dependence of the arising times of the local minima and maxima at the rotational revivals in the time-resolved high-harmonic spectra, the rotational gas temperature and the intensity of the pump laser has been extracted from the experiment. These parameters are then used to calculate the

*Corresponding author: cjin@njust.edu.cn

alignment distribution theoretically (see Sec. II E). Alternatively, it has been shown in Jin *et al.* [36] that the minima in the HHG spectra of aligned CO_2 molecules are very sensitive to the degree of alignment, which could be used to retrieve the degree of alignment. Very recently, Guo *et al.* [37] also suggested using the polarization properties of the harmonics from aligned molecules to retrieve the alignment distribution. In this later method, both the intensity ratio and the relative phase between the parallel and the perpendicular components of the harmonics as a function of the pump-probe angle are needed. But realistic measurement issues (small perpendicular component and efficiency of polarization measurement) limit the accuracy of this method. Since harmonic spectra from linear molecules are of great interest, here we propose an alternative method to obtain alignment distribution from the harmonic spectra of aligned CO_2 molecules.

Among molecules, CO_2 is one of the favorable candidates for investigating molecular HHG, it has attracted continuous and extensive interests in both experimental and theoretical studies [38–59]. Previous studies mostly focused on the two types of minima in the high-harmonic spectra, i.e., the "structural" minimum due to the photoionization cross section (PICS) of the highest occupied molecular orbital (HOMO) and the "dynamical" minimum caused by the interference of harmonics from the HOMO and from the inner molecular orbitals. Recently, it has been shown [36] that the discrepancy in the positions of the minima from two previous experiments on CO_2 [12,53,54] is due to the two experiments performed for molecules that have different alignment distributions. In drawing the conclusion, the theoretical calculations employed the quantitative rescattering (QRS) model [60–62] for harmonics from single molecules. To compare with experimental HHG spectra, the single-molecule complex dipoles were added coherently weighted by the alignment distribution, followed by the propagation of the harmonics in the gas medium by solving Maxwell's wave equations [63–65]. A prerequisite for the success of the model is the availability of accurate complex fixed-in-space PICS of CO_2 molecules which has been obtained by using the state-of-the-art quantum chemistry codes [66,67]. As a side product of the present calculations, we reevaluate an earlier experiment by Zhou *et al.* [68] where they demonstrated that elliptically polarized high harmonics of CO_2 molecules can be generated on aligned molecules using linearly polarized lasers. However, the measured intensity ratios between the parallel and perpendicular HHG components have not been successfully reproduced by the simulations so far [69]. Using the improved theory in this work, we also revisit this problem.

In this work, our main goals are twofold: first, we will simulate the intensity ratios between the perpendicular and the parallel components of harmonics generated from aligned CO_2 molecules to compare with the measured ones; second, by choosing the CO_2 as the target molecule, we propose a genetic-algorithm (GA) based iterative retrieval method to obtain the alignment distribution from "experimentally" measured harmonic spectra. In Sec. II we will give a brief introduction to our HHG theory, including the macroscopic propagation equations, the QRS model, and the coherent summation of the HHG from different molecular orbitals. In Sec. III we will first give the calculated macroscopic HHG spectra of aligned CO_2 molecules and the simulated intensity ratios between two harmonic components, which will be considered as "input" or "experimental" data; we will then demonstrate the GA-based retrieval method and test it under different conditions by using either the parallel and the perpendicular components of the HHG or the intensity ratio between them as a function of the pump-probe angle; finally we will show that the existence and location of minima in the HHG spectra would benefit the accuracy of the retrieval procedure. A summary will be given in Sec. IV.

II. THEORETICAL METHODS

To simulate the experimentally measured HHG from aligned molecules, three main steps are needed in the calculation. First, the HHG induced dipoles (including the amplitude and phase) of a fixed-in-space molecule from the HOMO and other inner orbitals, such as the HOMO-1 and HOMO-2, are individually computed by the QRS model, and they are then added up coherently. Second, together with the alignment distribution, the averaged induced dipoles of the molecules are calculated. Third, the averaged induced dipoles are served as the source of the three-dimensional Maxwell's wave equations of the high-harmonic field in the gas medium, in which macroscopic propagation and phase-matching effects are taken into account. Each of these steps will be described in the following. Based on the above-mentioned theoretical models, the calculated macroscopic HHG will be taken as "experimental" data from which the molecular alignment distribution will be retrieved.

A. The QRS model for a multiple-orbital molecular system

According to the QRS model, in the frequency domain, the induced dipole moment $D^{\parallel,\perp}(\omega,\theta)$ of a molecule at a fixed angle θ (defined with respect to the laser polarization direction) for a single molecular orbital is given by [60–62]

$$D^{\parallel,\perp}(\omega,\theta) = N(\theta)^{1/2} W(\omega) d^{\parallel,\perp}(\omega,\theta), \tag{1}$$

where $N(\theta)$ is the alignment-dependent ionization probability, $W(\omega)$ is the complex returning electron wave packet, and $d^{\parallel,\perp}(\omega,\theta)$ is the parallel or perpendicular component of the photorecombination (PR) transition dipole. Equation (1) is valid for the linearly polarized driving laser and linear molecules. $W(\omega)$ is the returning wave packet which reflects the properties of the driving laser only, thus it doesn't depend on the angle θ and it is the same for both harmonic components. It can be calculated by using either the strong-field approximation (SFA) or from the equivalent atomic target [60]:

$$W(\omega) = \frac{D^{\parallel,\perp}(\omega,\theta)}{N(\theta)^{1/2} d^{\parallel,\perp}(\omega,\theta)}. \tag{2}$$

If the HHG is caused not only by the HOMO but also the inner orbitals, the total laser-induced dipole moment of a fixed-in-space molecule can be calculated as

$$D_{\text{tot}}^{\parallel,\perp}(\omega,\theta) = \sum_j a_j D_j^{\parallel,\perp}(\omega,\theta) e^{i\phi_j}, \tag{3}$$

where index j refers to the molecular orbital, a_j is the electron occupation number of each molecular orbital, and ϕ_j is the ionization phase.

B. The coherently averaged induced dipole of aligned molecules

For transiently aligned molecules, the alignment distribution can be expressed as $\rho(\theta)$ in the pump-laser frame. If the angle between the polarization directions of the pump and probe lasers is α, the alignment distribution is transformed into a frame attached to the probe laser as [70]

$$\rho(\theta', \phi', \alpha) = \rho[\theta(\theta', \phi', \alpha)], \tag{4}$$

where θ' and ϕ' are defined in the probe-laser frame, and related to θ in the pump-laser frame as

$$\cos\theta = \cos\theta' \cos\alpha + \sin\theta' \sin\alpha \cos\phi'. \tag{5}$$

After coherently averaging the induced dipole moment over the molecular angular distribution, the averaged induced dipole can be obtained as [60,70]

$$\bar{D}_{\rm tot}^{\parallel,\perp}(\omega, \alpha) = \int_0^{2\pi} \int_0^{\pi} D_{\rm tot}^{\parallel,\perp}(\omega, \theta')\rho(\theta', \phi', \alpha) \sin\theta' d\theta' d\phi'. \tag{6}$$

C. Macroscopic propagation of the high-harmonic field in the medium

Under the conditions of low pressure and low laser intensity, the fundamental laser is not modified in the gas medium and can be expressed in an analytical form. We consider only the macroscopic propagation of high harmonics, which is described by the three-dimensional Maxwell's wave equation as [63,64,71]

$$\nabla^2 E_{\rm h}^{\parallel,\perp}(r, z, t, \alpha) - \frac{1}{c^2} \frac{\partial^2 E_{\rm h}^{\parallel,\perp}(r, z, t, \alpha)}{\partial^2 t} = \mu_0 \frac{\partial^2 P_{\rm nl}^{\parallel,\perp}(r, z, t, \alpha)}{\partial^2 t}. \tag{7}$$

Here $E_{\rm h}^{\parallel,\perp}(r, z, t, \alpha)$ and $P_{\rm nl}^{\parallel,\perp}(r, z, t, \alpha)$ are the parallel and perpendicular components of harmonic's electric field and the nonlinear polarization induced by the probe laser, respectively.

In Eq. (7) the nonlinear polarization term is given by

$$P_{\rm nl}^{\parallel,\perp}(r, z, t, \alpha) = [n_0 - n_{\rm e}(r, z, t, \alpha)]\bar{D}_{\rm tot}^{\parallel,\perp}(r, z, t, \alpha). \tag{8}$$

Here n_0 is the density of neutral molecules and the free-electron density $n_{\rm e}(t, \alpha)$ is calculated as

$$n_{\rm e}(t, \alpha) = \int_0^{2\pi} \int_0^{\pi} n_{\rm e}(t, \theta')\rho(\theta', \phi', \alpha) \sin\theta' d\theta' d\phi'. \tag{9}$$

In the above equation, $n_{\rm e}(t, \theta')$ is the alignment-dependent free-electron density and can be obtained from

$$n_{\rm e}(t, \theta') = n_0 \left\{ 1 - \exp\left[- \int_0^t \gamma(\tau, \theta') d\tau \right] \right\}, \tag{10}$$

where $\gamma(\tau, \theta')$ is the alignment-dependent ionization rate, given by the MO-ADK theory [72,73]. In Eq. (10) only the ionization from the HOMO is considered.

By going to a moving coordinate frame (i.e., $z' = z$, $t' = t - z/c$) and applying the paraxial approximation, Eq. (7) can be transferred to the frequency domain by a Fourier transform

$$\nabla_\perp^2 \widetilde{E}_{\rm h}^{\parallel,\perp}(r, z', \omega, \alpha) - \frac{2i\omega}{c} \frac{\partial \widetilde{E}_{\rm h}^{\parallel,\perp}(r, z', \omega, \alpha)}{\partial z'} = -\omega^2 \mu_0 \widetilde{P}_{\rm nl}^{\parallel,\perp}(r, z', \omega, \alpha), \tag{11}$$

with

$$\widetilde{E}_{\rm h}^{\parallel,\perp}(r, z', \omega, \alpha) = \hat{F}[E_{\rm h}^{\parallel,\perp}(r, z', t', \alpha)] \tag{12}$$

and

$$\widetilde{P}_{\rm nl}^{\parallel,\perp}(r, z', \omega, \alpha) = \hat{F}[P_{\rm nl}^{\parallel,\perp}(r, z', t', \alpha)], \tag{13}$$

where $\hat{F}$ is the Fourier transform operator acting on the temporal coordinate. Note that due to the convention in the Fourier transform the sign of $2i\omega/c$ in Eq. (11) is different from that in Ref. [71].

Finally, the spectra of parallel and perpendicular HHG components can be computed at the exit plane of the gas medium ($z' = z_{\rm out}$) as

$$S_h^{\parallel,\perp}(\omega, \alpha) \propto \int_0^{\infty} |\widetilde{E}_{\rm h}^{\parallel,\perp}(r, z', \omega, \alpha)|^2 2\pi r \, dr. \tag{14}$$

D. Averaged PR transition dipole embodied in the macroscopic HHG

The macroscopic HHG yields obtained from a single molecular orbital can be written as [63,74]

$$S_{\rm h}^{\parallel,\perp}(\omega, \alpha) \propto \omega^4 |W'(\omega)|^2 |\bar{d}^{\parallel,\perp}(\omega, \alpha)|^2, \tag{15}$$

where $W'(\omega)$ is the macroscopic wave packet, $\bar{d}^{\parallel,\perp}(\omega, \alpha)$ is the averaged PR transition dipole, which can be expressed as

$$\bar{d}^{\parallel,\perp}(\omega, \alpha) = \int_0^{2\pi} \int_0^{\pi} N(\theta')^{1/2} d^{\parallel,\perp}(\omega, \theta')\rho(\theta', \phi', \alpha) \sin\theta' d\theta' d\phi'. \tag{16}$$

Equations (15) and (16) form the theoretical basis for retrieving the alignment distribution from the macroscopic HHG spectra. For each harmonic, Eq. (15) shows that the macroscopic HHG signal is proportional to the modulus square of the averaged PR transition dipole, which is given by Eq. (16). Assuming that $N(\theta')$ and $d^{\parallel,\perp}(\omega, \theta')$ are known, $\rho(\theta)$ in the pump-laser frame is related to $\rho(\theta', \phi', \alpha)$ in Eq. (4), thus it can be retrieved from the pump-probe angle (α) dependence of a fixed macroscopic harmonic order.

E. Alignment distribution of molecules by a pump laser

The alignment distribution, or the rotational wave packet, of molecules excited by a relatively weak infrared laser (called as pump laser) interacting with linear molecules can be precisely calculated by solving the time-dependent Schrödinger equation (TDSE) [1,67]. Each molecule is treated as a rigid rotor. For each initial rotational state, the TDSE is

$$i\frac{\partial \Psi_{\rm JM}(\theta, \varphi, t)}{\partial t} = \left[B\mathbf{J}^2 - \frac{E_{\rm pump}(t)^2}{2}(\alpha_\parallel \cos^2\theta + \alpha_\perp \sin^2\theta) \right] \Psi_{JM}(\theta, \varphi, t), \tag{17}$$

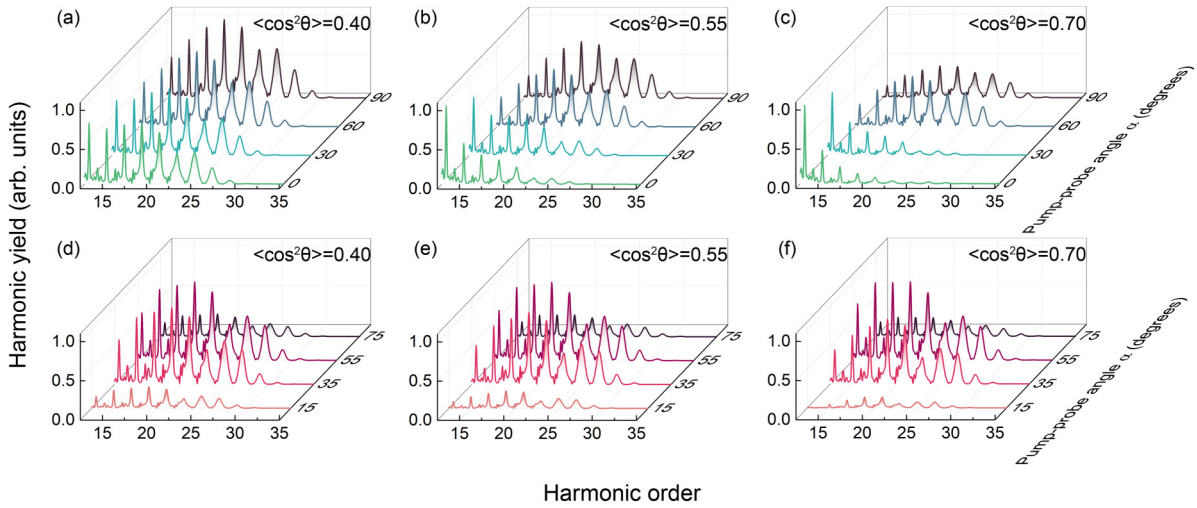

FIG. 1. The parallel (a–c) and perpendicular (d–f) components of the macroscopic HHG spectra from aligned CO_2 molecules at selected pump-probe angles. The alignment degrees $\langle\cos^2\theta\rangle$ are chosen at 0.40 (a, d), 0.55 (b, e), and 0.70 (c, f), respectively. Only harmonics from the HOMO is included. See text for other laser parameters.

where $E_{\rm pump}(t)$ is the electric field of the pump laser, $\mathbf{J}$ is the angular momentum operator, B is the rotational constant, and $\alpha_\parallel$ and $\alpha_\perp$ are the anisotropic polarizabilities in parallel and perpendicular directions with respect to the molecular axis, respectively.

Equation (17) is solved independently for each initial rotational state $|\mathrm{JM}\rangle$ using the split-operator method. After the pump laser is over, the rotational wave packet continues to propagate in the free space, and at the intervals of "rotational revivals" the molecules are nicely aligned or antialigned. The time-dependent rotational wave packet can be written as

$$\Psi_{\rm JM}(\theta,\varphi,t)=\sum_{\rm J'} a_{\rm J'}e^{-iE_{\rm J'}t}|\mathrm{J'M}\rangle, \tag{18}$$

where $E_{\rm J'}$ are eigenenergies, $|\mathrm{J'M}\rangle$ are spherical harmonics, and the coefficients $a_{\rm J'}$ are determined at the moment when the pump laser is off.

The time-dependent alignment distribution at a given gas temperature can be obtained by

$$\rho(\theta,t)=\sum_{\rm JM}\omega_{\rm JM}|\Psi_{\rm JM}(\theta,\varphi,t)|^2, \tag{19}$$

where $\omega_{\rm JM}$ is the weight according to the Boltzman distribution, in which the nuclear statistics and symmetry of the total electronic wave function are properly taken into account. The alignment distribution does not depend on the azimuthal angle φ for linear molecules.

III. RESULTS AND DISCUSSION

A. Macroscopic high harmonics of aligned CO_2 molecules

1. Simulated macroscopic high harmonics in the parallel and perpendicular directions

In the simulations, the alignment distribution of CO_2 molecules at the first half-revival (∼21.2 ps) is calculated by Eq. (19). The degree of alignment is defined with respect to the alignment distribution $\rho(\theta)$ in the pump-laser frame as

$$\langle\cos^2\theta\rangle=\int_0^\pi \cos^2\theta\ \rho(\theta)\sin\theta\, d\theta. \tag{20}$$

We first show some examples of the calculated macroscopic harmonic yields vs the pump-probe angle. The wavelength and the pulse duration of the probe laser are 800 nm and 15 fs. The beam waist at the laser focus is fixed at 35 μm, and a 0.5-mm-long gas jet is assumed with a uniform density distribution whose center is located 3 mm after the focus. The peak intensity of the probe laser is fixed as 1.5×10^{14} W/cm^2 at the center of the gas jet.

In Fig. 1 we show the simulated harmonic spectra as a function of the harmonic order (with respect to the 800-nm laser) in both parallel and perpendicular directions at some selected pump-probe angles. The degree of alignment $\langle\cos^2\theta\rangle$ is chosen to be 0.4, 0.55, and 0.7, respectively. The spectra are calculated from Eq. (14), and only the HOMO is included since the laser intensity is relatively low. The parallel or perpendicular harmonic yields are normalized with respect to the highest harmonic peak over the whole regions of the harmonic order and the pump-probe angle at each alignment degree, respectively. Note that the perpendicular harmonic component drops to zero when $\alpha=0^\circ$ or 90°. For the parallel harmonics, when the alignment degree $\langle\cos^2\theta\rangle=0.40$, the shapes of harmonic spectra are similar, and they don't change much by varying the angle α; see Fig. 1(a). As the alignment degree is increased, the harmonic spectra show a variety of spectral structures at different α; see Figs. 1(b) and 1(c). For the perpendicular component, the dependence of the harmonic spectra on the pump-probe angle does not change much by varying the degree of alignment; see Figs. 1(d)–1(f). The different behaviors of the parallel and perpendicular harmonics can be understood by the alignment-dependent differential PICSs of the HOMO, which can be found in Fig. 1 of Ref. [75].

Using the data in Fig. 1, we plot the harmonic yields (normalized using the maximum value of parallel harmonic at each order) as a function of the pump-probe angle in

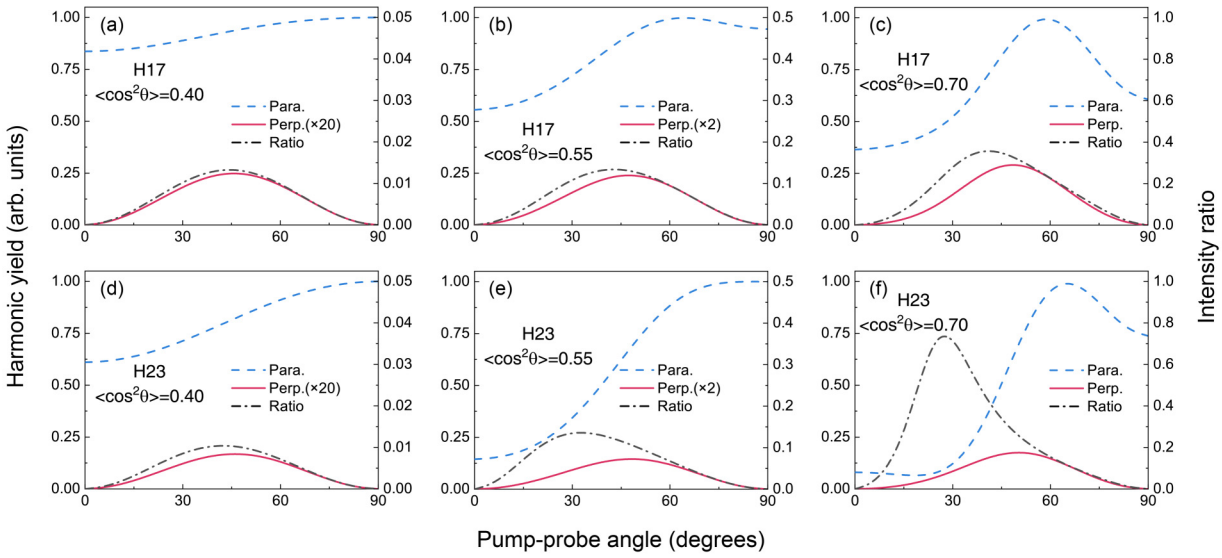

FIG. 2. The normalized HHG yields in the parallel (Para.) and perpendicular (Perp.) directions and the intensity ratios between them vs the pump-probe angle for H17 and H23, respectively. The results are shown at three different degrees of alignment. As indicated, some HHG data in the perpendicular direction are multiplied by some factors for easy comparison, and these factors are not included when calculating the intensity ratios.

Fig. 2 at the 17th harmonic order (H17) and H23, respectively. For the parallel harmonics, it is evident that the harmonic yields change slightly with the pump-probe angle α at the low alignment degree of 0.40 in Figs. 2(a) and 2(d), they change dramatically with α when $\langle\cos^2\theta\rangle$ is increased to the higher value of 0.55 (or 0.70) in Figs. 2(b) and 2(e) [or in Figs. 2(c) and 2(f)]. For the HHG in the perpendicular direction, the dependence of harmonic yields with α are similar at different alignment degrees. We also plot the intensity ratios between the perpendicular and the parallel harmonic components as a function of the pump-probe angle in Fig. 2. One can see that the variation of these ratios with α has a strong dependence on the degree of alignment. All of these simulated results in Fig. 2 are experimentally measurable quantities, which may be adopted to retrieve the alignment distribution.

2. *Comparison of the measured intensity ratios and the simulated ones*

We next check whether our simulations can reproduce the measurement for CO_2 molecules reported in Zhou *et al.* [68]. They measured the intensity ratios between the harmonic yields in two orthogonal directions versus the pump-probe angle when the CO_2 molecules are aligned at the half revival. Their results are shown in Fig. 3(a) for four harmonic orders. We choose the laser parameters close to those in Zhou *et al.*, and adjust the alignment degree $\langle\cos^2\theta\rangle$ to 0.48 so to best match the absolute values of the measured intensity ratios. The wavelength, duration, and peak intensity of the probe laser are 800 nm, 30 fs, and 1.9×10^{14} W/cm^2, respectively.

The simulated intensity ratios by only considering single-molecule response and the HOMO are shown in Fig. 3(b) calculated by using the QRS model from Eq. (6). The intensity ratios are not distinguishable between H17 and H19 (or H21 and H23). We have also checked that the sequence of peak intensity ratios corresponding to each harmonic order changes randomly by slightly changing the laser intensity. Similar simulations have been performed by Le *et al.* [69] with a higher alignment degree. In our simulation and Le *et al.*, based on the single-molecule theory, the results are not in good agreement with the experiment. We next include the propagation effect in the simulation, and keep other macroscopic parameters the same as those in Fig. 1. The resulting

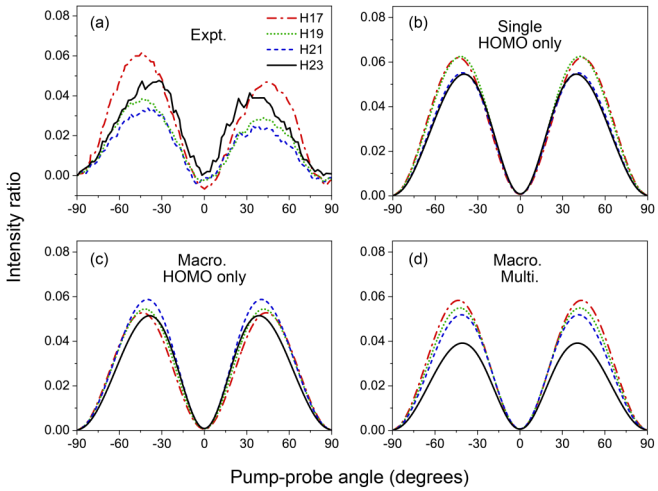

FIG. 3. The intensity ratio between the perpendicular and parallel HHG components as a function of the pump-probe angle for H17 to H23. (a) The experimental (Expt.) results are taken from Zhou *et al.* [68]. (b–d) The simulated results. In (b) the single-molecule response is calculated by including only contribution from the HOMO. In (c) and (d) the macroscopic (Macro.) propagation simulations are carried out by including contribution from the HOMO only and by including multiple (Multi.) orbital interference of the HOMO with HOMO-1 and HOMO-2, respectively. The alignment degree is $\langle\cos^2\theta\rangle = 0.48$.

intensity ratios are plotted in Fig. 3(c). The values of the intensity ratios changed with the pump-probe angle become indistinguishable for different harmonic orders, which are definitely different from the measured ones. Finally, we perform the macroscopic propagation calculations by including the interference of the HOMO with HOMO-1 and HOMO-2. A nonzero relative phase between the two molecular orbitals would reflect nonadiabatic dynamics of electron rearrangement during the strong-field ionization, which is sensitive to laser intensity [27]. In Ref. [27] the relative ionization phase between HOMO and HOMO-2 of CO_2 molecules is chosen to be $-\pi/2$ at a high laser intensity to correctly predict the positions of the experimentally measured minima in the HHG spectra. According to the convention of Fourier transform in this work, we have chosen $\phi_{\text{HOMO-2}} - \phi_{\text{HOMO}} = \pi/2$ in Eq. (3), and it has been chosen as $\phi_{\text{HOMO-1}} - \phi_{\text{HOMO}} = -\pi/2$ because of symmetry of the molecular orbital. A much better agreement with the measurement is achieved in Fig. 3(d). The curves for intensity ratios at different orders can be clearly distinguished from each other. The peak value of intensity ratio decreases gradually from H17 to H21, and for H23 its peak value is very close to the measured one. However, the abnormal large value of H23 located between H17 and H19 curves in the experiment is still not reproduced by our simulation. Note that the peak value of the intensity ratio changes monotonically with the harmonic order for aligned N_2 molecules in Zhou *et al.* [68], which has been successfully reproduced by our HHG theory [37]. Could the discrepancy be due to other effects that are not included in the QRS theory, like nuclear vibrations, hole dynamics, or electron-electron correlation? On the other hand, the measured intensity ratios are symmetric with respect to 0° for aligned N_2 molecules, but not for aligned CO_2 molecules in Zhou *et al.* [68]. It may be of interest to carry out additional independent experiments on CO_2, and also extending measurement to other linear molecules, like O_2, N_2O, and C_2H_2 [53,54,76,77], since such measurements are rare.

B. Retrieval of molecular alignment distribution using the genetic algorithm

For the cylindrically symmetric CO_2 molecules, the alignment distribution function $\rho(\theta)$ can be expanded as a polynomial of $\cos^2\theta$:

$$\rho(\theta) = a_0 + \sum_{n=1}^{n_{\max}} a_n \cos^{2n}\theta, \tag{21}$$

where a_n ($n = 0,\ldots, n_{\max}$) is the expansion coefficient. Thus to retrieve the alignment distribution is actually to determine these coefficients.

We choose the genetic algorithm (GA) to obtain the parameters of $\{a_n\}$ in Eq. (21). GA is one of the established evolutionary algorithms that can deal with highly nonlinear response functions and has been widely applied to study strong-field phenomena [78–80]. It starts with a population of randomly generated individuals, and better individuals are selected from the current generation by evaluating the fitness function of each individual which are then used in the next generation. Once a satisfactory fitness level is reached, the evolution process is terminated. In our retrieval method, we use the harmonic yields versus the pump-probe angle at a fixed harmonic order to construct the fitness function, which is defined as

$$F\{a_n\} = \sum_i |S_{\text{input}}(\alpha_i) - S_{\text{retrieval}}(\alpha_i)|^2, \tag{22}$$

where i is the index of the pump-probe angle α, S_{input} are the input data, and $S_{\text{retrieval}}$ are the calculated ones by using one set of $\{a_0, a_1, \ldots, a_{n_{\max}}\}$. We also set constraints for the alignment distribution in the optimization procedure. For example, it should satisfy the normalization condition of $\int_0^\pi \rho(\theta)\sin\theta\, d\theta = 1$. Note that, as shown in Fig. 4, real alignment distribution always peaks at 0° and decreases monotonically with increasing alignment angle till 90°. Finally, by minimizing $F\{a_n\}$, multiple parameters can be searched and optimized.

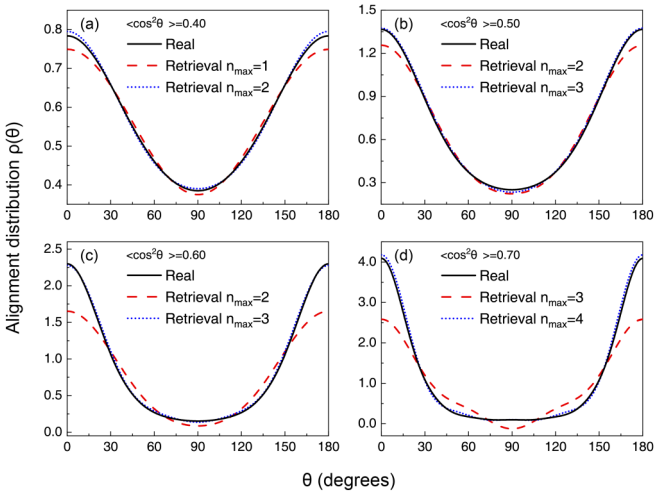

FIG. 4. Molecular alignment distribution function $\rho(\theta)$ of aligned CO_2 molecules retrieved by using the intensity ratio of the two polarization components of H17. Contribution is from the HOMO only in the single-molecule response. The wavelength, duration, and intensity of the probe laser are 800 nm, 15 fs, and 2.0 $\times$ 10^{14} W/cm^2. The different $n_{\max}$ indicated is required for the different alignment degree of $\langle\cos^2\theta\rangle$ in the retrieval.

We use the intensity ratios between the two HHG components at H17 as "input" data to check the validity of our retrieval method. These data are calculated with Eq. (6) by using the single-molecule QRS model with the contribution from the HOMO only and by varying the pump-probe angle with a step of 5°. With the known alignment-dependent ionization probability and the PR transition dipoles of CO_2 molecules, the retrieved alignment distributions are plotted in Fig. 4. For comparison, the "input" (or "real") alignment distributions are also shown. For each given degree of the alignment, if the required $n_{\max}$ (or the number of expansion terms) is big enough, its angular distribution can be accurately retrieved. The higher the degree of alignment, the bigger the $n_{\max}$ is needed. For example, at least five expansion coefficients are needed for $\langle\cos^2\theta\rangle = 0.70$. Since GA has the ability to handle a large number of unknown parameters, our retrieval method works for the alignment degree higher than 0.70.

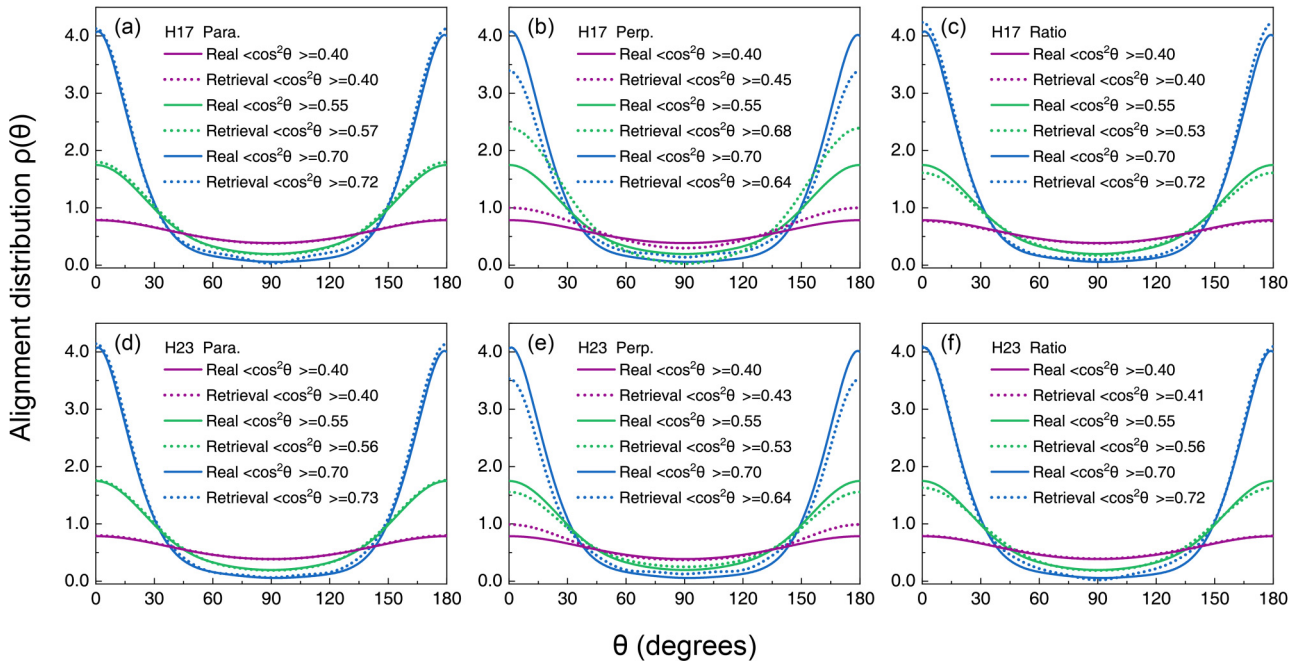

FIG. 5. Comparison of the real and the retrieved alignment distributions and alignment degrees $\langle\cos^2\theta\rangle$. Retrieved ones are obtained by using the simulated macroscopic high harmonics (H17 and H23) with the contribution from the HOMO as the "experimental" data. In the retrieval the laser intensity is taken at $1.5 \times 10^{14}\,\mathrm{W/cm^2}$ for calculating the alignment-dependent ionization probability $N(\theta)$, $n_{\max} = 3$ for $\langle\cos^2\theta\rangle = 0.40$ and 0.55, and $n_{\max} = 5$ for $\langle\cos^2\theta\rangle = 0.70$.

For the retrieval examples in this work, we limit $n_{\max}$ to less or equal to 5.

C. Retrieval of molecular alignment distribution using simulated macroscopic HHG spectra as "experimental" data

1. Comparison of retrieved alignment distributions from different harmonics

In this section we take the simulated macroscopic high harmonics as "experimental" data to retrieve alignment distribution of CO_2 molecules. These data are obtained at a relatively low laser intensity such that contributions from inner orbital electrons can be neglected, see Fig. 2. We choose harmonic yields in the parallel and perpendicular directions, as well as their intensity ratios. In the retrieval, the modulus square of the averaged PR transition dipole in Eq. (16) is calculated instead of the macroscopic HHG. For two harmonic orders H17 and H23, the retrieved alignment distributions are plotted in Fig. 5, and the known input alignment distributions are also plotted for comparison. Furthermore, the known and retrieved alignment degrees $\langle\cos^2\theta\rangle$ are indicated in the figures. In the retrieval, we start with several random sets of parameters such that a number of optimized sets can be obtained after thousands of generation. We locate the parameter set that gives the smallest value of the fitness function which gives the best match to the "real" alignment distribution. For different $\langle\cos^2\theta\rangle$ and different harmonic orders, the retrieved distributions agree very well with the "real" ones if the parallel high harmonics or the intensity ratios versus the pump-probe angles are employed in the retrieval. The largest relative error in $\langle\cos^2\theta\rangle$ is not larger than 4%. However, if the perpendicular high harmonics are used, then the retrieved distributions

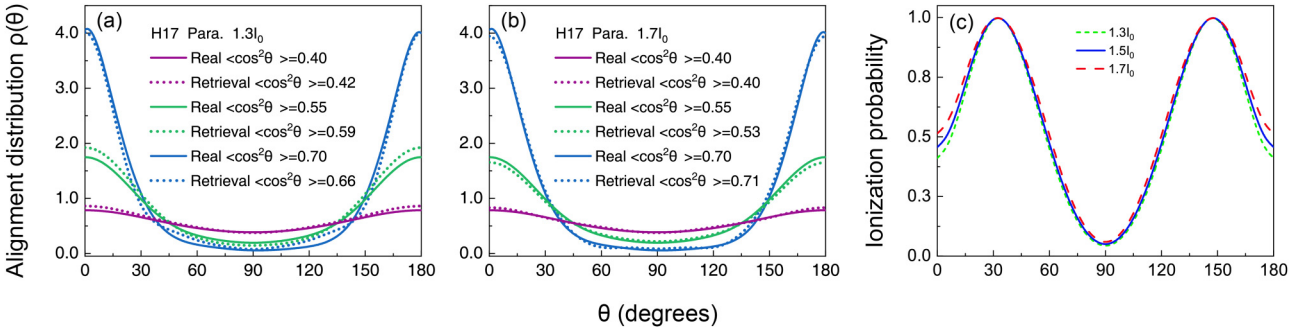

FIG. 6. (a, b) Same as Fig. 5 except that the laser intensity is $1.3I_0$ or $1.7I_0$ in the retrieval. Here $I_0 = 1.0 \times 10^{14}\,\mathrm{W/cm^2}$. (c) The dependence of the ionization probability (normalized, at the end of the probe pulse) on the alignment angle θ calculated by using the MO-ADK theory [72,73]. Laser wavelength and duration are 800 nm and 15 fs, and laser peak intensity is indicated in the figure.

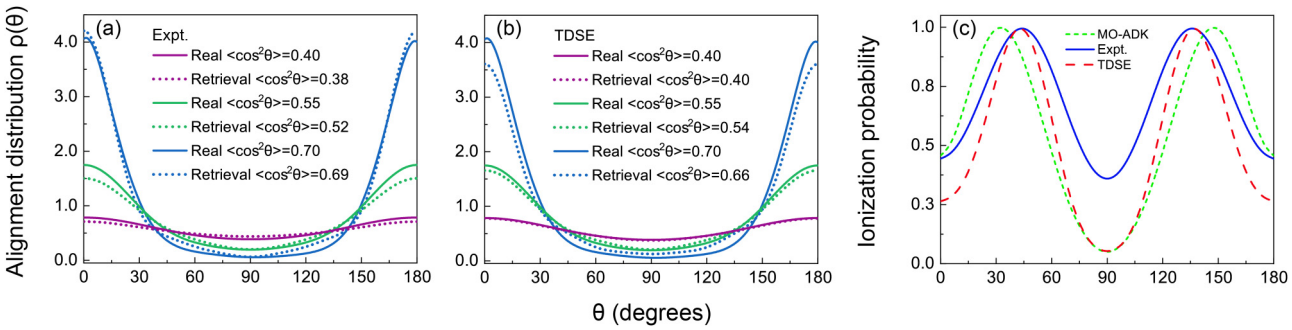

FIG. 7. (a, b) Retrieved alignment distributions and alignment degrees in comparison with real ones by using simulated macroscopic HHG yields (H17, parallel component) in Fig. 2. (c) Alignment-dependent ionization probabilities (normalized) from experiment (blue solid line) [82] and from TDSE calculation (red dashed line) [83], which are employed in the retrieval procedure. The ionization data from MO-ADK theory (green dotted line) is also shown for comparison.

deviate much more from the "real" ones. This can be understood from Fig. 2, where the dependence of the normalized harmonic yields on the pump-probe angle is insensitive to the change of the degree of alignment. In the following, we choose only the parallel high harmonics in the retrieval.

2. *Sensitivity of the retrieved alignment distributions on errors in the angular ionization probability*

In our retrieval method, the laser intensity is assumed known, which is used to calculate the alignment-dependent ionization probability $N(\theta)$. However, this parameter is rarely measured precisely in the experiment. Can the alignment distribution be correctly retrieved if the laser intensity has some uncertainties? We again use the parallel H17 harmonics in Fig. 2 as our "experimental" data. In the retrieval, the laser intensity is assumed as $1.3 \times 10^{14}\,\mathrm{W/cm^2}$ or $1.7 \times 10^{14}\,\mathrm{W/cm^2}$. The retrieved results are shown in Fig. 6. By introducing about 13% error in the laser intensity, the retrieved alignment distributions mostly agree with the "real" ones except for some discrepancies near 0° and 180°. The biggest relative error of the retrieved alignment degree with respect to the "real" one is about 7% and 4% in Figs. 6(a) and 6(b), respectively. Such increased error in the retrieved results can be understood from the alignment-dependent ionization probability plotted in Fig. 6(c). For three laser intensities, the ionization probabilities are normalized at their maximum values to easily see their different dependence on the alignment angle θ, which is one of the key parts in the retrieval.

In our retrieval, the alignment-dependent ionization probability is calculated from the MO-ADK theory. However, for CO_2, the prediction of the MO-ADK theory has been shown to have some discrepancies [81] from the experiment of Thomann *et al.* [82] and the TDSE calculation of Abu-samha and Madsen [83], especially its peak position; see Fig. 7(c). We then check how sensitive the retrieved alignment distribution is if the angular ionization probability is taken from the experiment and from the TDSE results. We still use the parallel macroscopic HHG yields (H17) in Fig. 2 as our "experimental" data. The retrieved results are shown in Figs. 7(a) and 7(b), which are generally in good agreement with the "real" ones. The maximum relative error in $\langle\cos^2\theta\rangle$ is less than 6%. Thus our retrieval method is not sensitive to errors in the alignment-dependent ionization probability.

3. *Influence of multi-orbital interference on the retrieved alignment distributions*

If the laser intensity of the probe laser is increased, both the HOMO and inner molecular orbitals could contribute to the HHG process. Can the alignment distribution still be well retrieved solely by relying on the single-orbital theory in Eq. (14)? We first simulate the macroscopic parallel high harmonics (H17 and H23) by setting the laser intensity at the center of gas medium at $2.0 \times 10^{14}\,\mathrm{W/cm^2}$ but keeping the other laser and gas parameters the same as those in Fig. 1. In the simulations, all the HOMO, HOMO-1, and HOMO-2 are included. The simulated harmonics are treated as "input" ones. The retrieved alignment distributions and alignment degrees are shown in Fig. 8. Generally speaking, the shapes of alignment distributions can be reproduced reasonably well at different degrees of alignment by using two different harmonic orders. With the increase of alignment degree, the error in the retrieved alignment degree becomes bigger, but it is still within 10%.

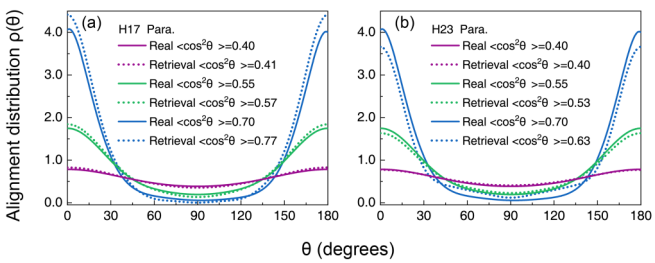

FIG. 8. Comparison of real and retrieved alignment distributions and alignment degrees. The macroscopic high harmonics (H17 and H23) in the parallel direction with the contribution from three outmost molecular orbitals are served as "experimental" ones. The intensity of the probe laser in the retrieval is $2.0 \times 10^{14}\,\mathrm{W/cm^2}$.

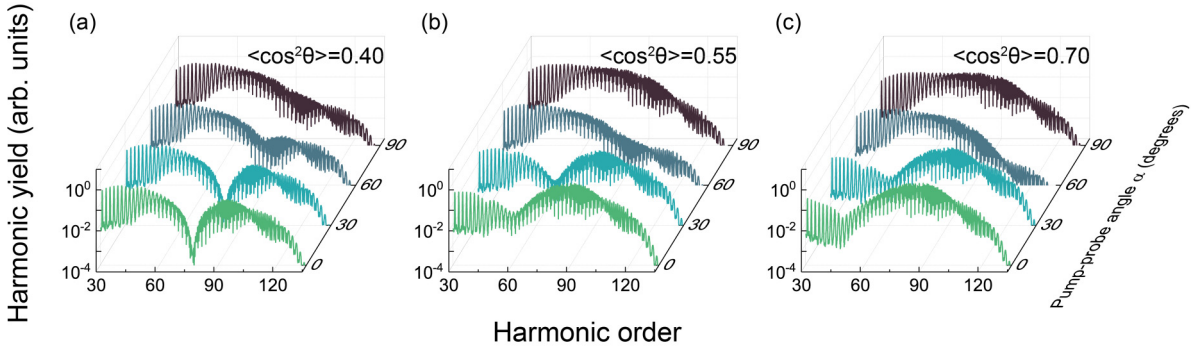

FIG. 9. The macroscopic parallel HHG spectra generated by the 1600-nm probe lasers at selected pump-probe angles. The alignment degree $\langle\cos^2\theta\rangle = 0.40$ (a), 0.55 (b), and 0.70 (c). See text for other simulation parameters.

4. The minimum in the HHG spectrum of CO_2 molecules and its influence on the retrieved alignment distribution

In the above discussion, the high harmonics are limited in the region of low photon energies due to the short wavelength of the probe laser. Extending photon energy to 40–70 eV, previous experiments [12,54] and theories [36,64,75] have shown rich spectral features in the high harmonics, in particular, the conspicuous minima for aligned CO_2 molecules. Can these features be used to enhance the precision of the retrieved alignment distribution?

To answer the above question, we first look at the simulated macroscopic HHG spectra in the parallel direction generated by 1600-nm lasers in Fig. 9. The peak intensity of the probe laser (at the center of gas medium) is 1.0×10^{14} W/cm^2 and the other conditions are the same as those in Fig. 1. Only the HOMO contribution is included in the simulation. Here the harmonic order is defined with respect to the 1600-nm laser. At the low alignment of $\langle\cos^2\theta\rangle = 0.40$, a deep minimum occurs around H77 (i.e., 60 eV) for small pump-probe angles. This deep minimum is directly related to the minimum in the averaged transition dipole, whose origin has been explained in Ref. [75]. At higher alignment of $\langle\cos^2\theta\rangle = 0.55$ and 0.70, the minimum becomes shallower and its position changes rapidly with the pump-probe angle.

We next plot the harmonic yield versus the pump-probe angle at three selected harmonic orders in Fig. 10. For H51, there is no minimum for three alignments shown. For H75, the minimum occurs only for two higher alignments. For H79, the minimum always appears, and its position shifts (in the pump-probe angle) with the change of alignment. We choose the harmonic yields for H51 and H79 as "experimental" data to retrieve the alignment distributions. The retrieved results are shown in Fig. 11. The retrieved alignment distributions in Fig. 11(a) from H51 are in very good agreement with the "real" ones, and the largest relative error in $\langle\cos^2\theta\rangle$ is less than 3%. If H79 is used, both the alignment distribution and $\langle\cos^2\theta\rangle$ are perfectly retrieved [see Fig. 11(b)], which is almost identical to the "real" distribution, no matter whether the degree of alignment is high or low. From these results, we can conclude that conspicuous minimum structures in the pump-probe angle-dependent harmonic spectra are favorable for the accurate retrieval of the molecular alignment distribution.

Before closing, we further address a realistic measurement issue about the minimum in the harmonic spectrum. As shown in Fig. 12(a), the harmonic yields in Fig. 10(c) are plotted on logarithmic scale, thus very deep minima (solid lines) can be easily seen. In our recent investigation on the minima in the measured HHG spectra of aligned CO_2 molecules [36], the positions of the minima are correctly reproduced, but the measured minima are much shallower than those predicted from the theory. Clear deep minima can be compromised by the limited sensitivity of the spectrometer, or probably the presence of perpendicular component of the harmonics. Does the depth of the minimum affect the retrieved alignment distribution? To test this concern, we fix the positions of the

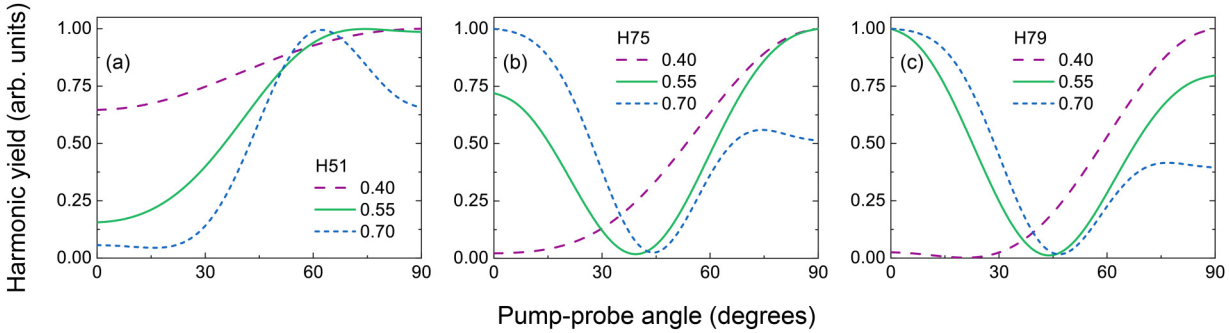

FIG. 10. The parallel harmonic yields (normalized) vs the pump-probe angle for three orders (H51, H75, and H79) at different alignment degrees.

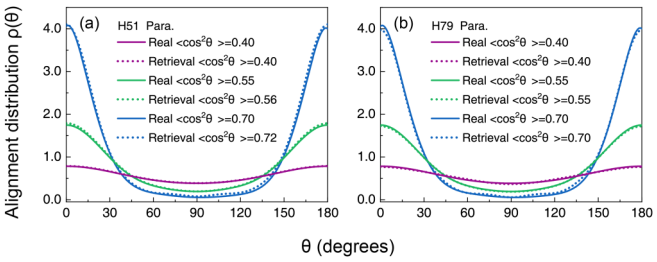

FIG. 11. Real and retrieved alignment distributions and alignment degrees. "Input" data are taken from Fig. 10(a) for H51 and from Fig. 10(c) for H79.

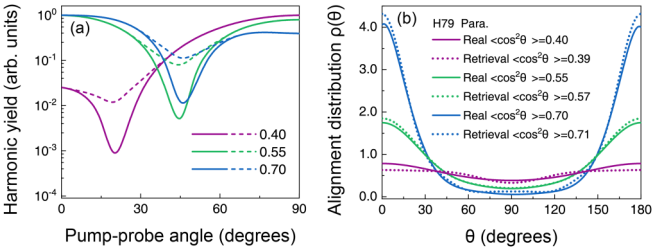

FIG. 12. (a) Harmonic yields of H79 as a function of the pump-probe angle replotted from Fig. 10(c) (solid lines) and modified around the minima (dashed lines). (b) Comparison of real and retrieved alignment data.

minima and artificially making the depth to be shallower. The "tweaked" spectra are shown with dashed lines in Fig. 12(a), and they are regarded as "input" data. The retrieved alignment data are shown in Fig. 12(b). For the alignment of $\langle\cos^2\theta\rangle$ from 0.40 to 0.70, the retrieved alignment distributions are all in very good agreement with the "real" ones. Thus the sharpness of the minimum does not affect the accuracy of the retrieved results.

IV. CONCLUSIONS

In the past two decades, high-order harmonic spectra from aligned CO_2 molecules have been extensively studied in many experiments and theories. With improved experimental technology and advance in theories, the focus of studying HHG is no longer limited to understanding the high harmonic spectrum only, but rather what structure details of the molecule itself can be extracted from such experiment.

In this article, we addressed two issues. First, we revisited the experimental results in Zhou *et al.* [68] where parallel and perpendicular components of the harmonics from aligned CO_2 molecules have been reported. In an earlier paper, Le *et al.* [69] used the QRS theory to look into this experiment, but only under the single molecule model. With the theoretical tools available, it is desirable to perform calculations that account for all factors that can contribute to the experimental results. The list includes effects of the multi-orbital interference, average over the alignment distribution, and account for macroscopic propagation of harmonics in the gas medium. With these factors included, the agreement with the results in Zhou *et al.* [68] has improved, but some discrepancies remain. Polarization measurements for high harmonics are still rare for harmonic spectra and additional experiments might reveal new challenges.

Second, we proposed a method to retrieve the molecular alignment distribution from the measured harmonic spectra using the genetic algorithm. To construct a complete theory for experimentally observed harmonic spectra from aligned molecules, information about the alignment distribution is required. If this distribution is known accurately, then starting with the QRS theory, all the ingredients for carrying out calculations that account for all the processes that lead to the experimentally observed HHG are available, including the accurate photo-recombination transition dipoles. In the second topic of this article, we demonstrated that the parallel harmonic yields or the intensity ratios between the parallel and the perpendicular HHG can be used to obtain more accurate alignment distributions, even if there are some uncertainties in the alignment-dependent ionization probability or when HOMO and inner molecular orbitals are contributing to the HHG. We also examined that the minima in the HHG spectra driven by the long-wavelength lasers are even better for retrieving accurate alignment distribution. The ubiquitous presence of pronounced minima in the harmonic spectra in the 40–70 eV range driven by long-wavelength laser offers a more sensitive and accurate retrieval of the alignment distribution.

Looking ahead, it would be of great interest to look into the possibility of generalizing this method to nonlinear molecules. This probably will not occur anytime soon since retrieval is an inverse scattering problem. Harmonic spectra for nonlinear molecules have not been widely studied so far. Within the linear molecules, perhaps the present method can be extended to study aligned molecules that are vibrationally excited as well.

ACKNOWLEDGMENTS

This work was supported by National Natural Science Foundation of China (NSFC) under Grants No. 91950102, No. 11774175, and No. 11834004. C.D.L. was supported by Chemical Sciences, Geosciences and Biosciences Division, Office of Basic Energy Sciences, Office of Science, U.S. Department of Energy under Grant No. DE-FG02-86ER13491.

[1] H. Stapelfeldt and T. Seideman, Rev. Mod. Phys. **75**, 543 (2003).
[2] C. P. Koch, M. Lemeshko, and D. Sugny, Rev. Mod. Phys. **91**, 035005 (2019).
[3] B. Friedrich and D. Herschbach, Phys. Rev. Lett. **74**, 4623 (1995).
[4] L. Cai, J. Marango, and B. Friedrich, Phys. Rev. Lett. **86**, 775 (2001).
[5] O. Ghafur, A. Rouzée, A. Gijsbertsen, W. K. Siu, S. Stolte, and M. J. J. Vrakking, Nat. Phys. **5**, 289 (2009).
[6] X. Ren, V. Makhija, and V. Kumarappan, Phys. Rev. Lett. **112**, 173602 (2014).

[7] K. Lin, I. Tutunnikov, J. Qiang, J. Ma, Q. Song, Q. Ji, W. Zhang, H. Li, F. Sun, X. Gong *et al.*, Nat. Commun. **9**, 5134 (2018).

[8] H. Ihee, V. A. Lobastov, U. M. Gomez, B. M. Goodson, R. Srinivasan, C.-Y. Ruan, and A. H. Zewail, Science **291**, 458 (2001).

[9] Y. Mairesse, J. Higuet, N. Dudovich, D. Shafir, B. Fabre, E. Mével, E. Constant, S. Patchkovskii, Z. Walters, M. Y. Ivanov, and O. Smirnova, Phys. Rev. Lett. **104**, 213601 (2010).

[10] B. K. McFarland, J. P. Farrell, P. H. Bucksbaum, and M. Gühr, Science **322**, 1232 (2008).

[11] J. Itatani, J. Levesque, D. Zeidler, H. Niikura, H. Pépin, J.-C. Kieffer, P. B. Corkum, and D. M. Villeneuve, Nature (London) **432**, 867 (2004).

[12] C. Vozzi, M. Negro, F. Calegari, G. Sansone, M. Nisoli, S. De Silvestri, and S. Stagira, Nat. Phys. **7**, 822 (2011).

[13] C. I. Blaga, J. Xu, A. D. DiChiara, E. Sistrunk, K. Zhang, P. Agostini, T. A. Miller, L. F. DiMauro, and C. D. Lin, Nature (London) **483**, 194 (2012).

[14] M. G. Pullen, B. Wolter, A.-T. Le, M. Baudisch, M. Hemmer, A. Senftleben, C. D. Schröter, J. Ullrich, R. Moshammer, C. D. Lin *et al.*, Nat. Commun. **6**, 7262 (2015).

[15] D. Pavičić, K. F. Lee, D. M. Rayner, P. B. Corkum, and D. M. Villeneuve, Phys. Rev. Lett. **98**, 243001 (2007).

[16] J. Ortigoso, M. Rodrıguez, M. Gupta, and B. Friedrich, J. Chem. Phys. **110**, 3870 (1999).

[17] C. Cornaggia, Phys. Rev. A **91**, 043426 (2015).

[18] F. Rosca-Pruna and M. J. J. Vrakking, Phys. Rev. Lett. **87**, 153902 (2001).

[19] P. W. Dooley, I. V. Litvinyuk, K. F. Lee, D. M. Rayner, M. Spanner, D. M. Villeneuve, and P. B. Corkum, Phys. Rev. A **68**, 023406 (2003).

[20] I. Bocharova, R. Karimi, E. F. Penka, J.-P. Brichta, P. Lassonde, X. Fu, J.-C. Kieffer, A. D. Bandrauk, I. Litvinyuk, J. Sanderson, and F. Légaré, Phys. Rev. Lett. **107**, 063201 (2011).

[21] K. Mizuse, K. Kitano, H. Hasegawa, and Y. Ohshima, Sci. Adv. **1**, e1400185 (2015).

[22] X. M. Tong, Z. X. Zhao, A. S. Alnaser, S. Voss, C. L. Cocke and C. D. Lin, J. Phys. B **38**, 333 (2005).

[23] P. Dietrich, D. T. Strickland, M. Laberge, and P. B. Corkum, Phys. Rev. A **47**, 2305 (1993).

[24] K. J. Schafer, B. Yang, L. F. DiMauro, and K. C. Kulander, Phys. Rev. Lett. **70**, 1599 (1993).

[25] P. B. Corkum, Phys. Rev. Lett. **71**, 1994 (1993).

[26] N. L. Wagner, A. Wüest, I. P. Christov, T. Popmintchev, X. Zhou, M. M. Murnane, and H. C. Kapteyn, Proc. Natl. Acad. Sci. U. S. A. **103**, 13279 (2006).

[27] O. Smirnova, Y. Mairesse, S. Patchkovskii, N. Dudovich, D. Villeneuve, P. Corkum, and M. Y. Ivanov, Nature (London) **460**, 972 (2009).

[28] W. Li, X. Zhou, R. Lock, S. Patchkovskii, A. Stolow, H. C. Kapteyn, and M. M. Murnane, Science **322**, 1207 (2008).

[29] H. J. Wörner, J. B. Bertrand, D. V. Kartashov, P. B. Corkum, and D. M. Villeneuve, Nature (London) **466**, 604 (2010).

[30] V.-H. Le, A.-T. Le, R.-H. Xie, and C. D. Lin, Phys. Rev. A **76**, 013414 (2007).

[31] S. Haessler, J. Caillat, W. Boutu, C. Giovanetti-Teixeira, T. Ruchon, T. Auguste, Z. Diveki, P. Breger, A. Maquet, B. Carré *et al.*, Nat. Phys. **6**, 200 (2010).

[32] X. Zhu, M. Qin, Y. Li, Q. Zhang, Z. Xu, and P. Lu, Phys. Rev. A **87**, 045402 (2013).

[33] C. Zhai, X. Zhu, P. Lan, F. Wang, L. He, W. Shi, Y. Li, M. Li, Q. Zhang, and P. Lu, Phys. Rev. A **95**, 033420 (2017).

[34] Y. He, L. He, P. Lan, B. Wang, L. Li, X. Zhu, W. Cao, and P. Lu, Phys. Rev. A **99**, 053419 (2019).

[35] Y. He, L. He, P. Wang, B. Wang, S. Sun, R. Liu, B. Wang, P. Lan, and P. Lu, Opt. Express **28**, 21182 (2020).

[36] C. Jin, S.-J. Wang, X. Zhao, S.-F. Zhao, and C. D. Lin, Phys. Rev. A **101**, 013429 (2020).

[37] X. Guo, C. Jin, Z. He, J. Yao, X.-X. Zhou, and Y. Cheng, Opt. Express **29**, 1613 (2021).

[38] M. Lein, N. Hay, R. Velotta, J. P. Marangos, and P. L. Knight, Phys. Rev. Lett. **88**, 183903 (2002).

[39] R. de Nalda, E. Heesel, M. Lein, N. Hay, R. Velotta, E. Springate, M. Castillejo, and J. P. Marangos, Phys. Rev. A **69**, 031804(R) (2004).

[40] T. Kanai, S. Minemoto, and H. Sakai, Nature (London) **435**, 470 (2005).

[41] C. Vozzi, F. Calegari, E. Benedetti, J.-P. Caumes, G. Sansone, S. Stagira, M. Nisoli, R. Torres, E. Heesel, N. Kajumba, J. P. Marangos, C. Altucci, and R. Velotta, Phys. Rev. Lett. **95**, 153902 (2005).

[42] A.-T. Le, X.-M. Tong, and C. D. Lin, Phys. Rev. A **73**, 041402(R) (2006).

[43] M. Gühr, B. K. McFarland, J. P. Farrell, and P. H. Bucksbaum, J. Phys. B **40**, 3745 (2007).

[44] N. Wagner, X. Zhou, R. Lock, W. Li, A. Wüest, M. Murnane, and H. Kapteyn, Phys. Rev. A **76**, 061403(R) (2007).

[45] Y. J. Chen and J. Liu, Phys. Rev. A **77**, 013410 (2008).

[46] W. Boutu, S. Haessler, H. Merdji, P. Breger, G. Waters, M. Stankiewicz, L. Frasinski, R. Taieb, J. Caillat, and A. Maquet, Nat. Phys. **4**, 545 (2008).

[47] X. Zhou, R. Lock, W. Li, N. Wagner, M. M. Murnane, and H. C. Kapteyn, Phys. Rev. Lett. **100**, 073902 (2008).

[48] T. Kanai, E. J. Takahashi, Y. Nabekawa, and K. Midorikawa, Phys. Rev. A **77**, 041402(R) (2008).

[49] P. Wei, P. Liu, J. Chen, Z. Zeng, X. Guo, X. Ge, R. Li, and Z. Xu, Phys. Rev. A **79**, 053814 (2009).

[50] R. Torres, T. Siegel, L. Brugnera, I. Procino, J. G. Underwood, C. Altucci, R. Velotta, E. Springate, C. Froud, I. C. E. Turcu *et al.*, Phys. Rev. A **81**, 051802(R) (2010).

[51] H. J. Wörner, J. B. Bertrand, P. Hockett, P. B. Corkum, and D. M. Villeneuve, Phys. Rev. Lett. **104**, 233904 (2010).

[52] K. Kato, S. Minemoto, and H. Sakai, Phys. Rev. A **84**, 021403(R) (2011).

[53] A. Rupenyan, P. M. Kraus, J. Schneider, and H. J. Wörner, Phys. Rev. A **87**, 033409 (2013).

[54] A. Rupenyan, P. M. Kraus, J. Schneider, and H. J. Wörner, Phys. Rev. A **87**, 031401(R) (2013).

[55] M. Qin, X. Zhu, Y. Li, Q. Zhang, P. Lan, and P. Lu, Opt. Express **22**, 6362 (2014).

[56] H. Yun, K.-M. Lee, J. H. Sung, K. T. Kim, H. T. Kim, and C. H. Nam, Phys. Rev. Lett. **114**, 153901 (2015).

[57] B. D. Bruner, Z. Mašín, M. Negro, F. Morales, D. Brambila, M. Devetta, D. Faccialà, A. G. Harvey, M. Ivanov, Y. Mairesse *et al.*, Faraday Discuss. **194**, 369 (2016).

[58] N. Suárez, A. Chacón, J. A. Pérez-Hernández, J. Biegert, M. Lewenstein, and M. F. Ciappina, Phys. Rev. A **95**, 033415 (2017).

[59] M. Ruberti, P. Decleva, and V. Averbukh, Phys. Chem. Chem. Phys. **20**, 8311 (2018).

[60] A.-T. Le, R. R. Lucchese, S. Tonzani, T. Morishita, and C. D. Lin, Phys. Rev. A **80**, 013401(R) (2009).
[61] C. D. Lin, A.-T. Le, C. Jin, and H. Wei, J. Phys. B **51**, 104001 (2018).
[62] C. D. Lin, C. Jin, A.-T. Le, and H. Wei, *Attosecond and Strong-Field Physics: Principles and Applications* (Cambridge University Press, Cambridge, 2018).
[63] C. Jin, A.-T. Le, and C. D. Lin, Phys. Rev. A **79**, 053413 (2009).
[64] C. Jin, A.-T. Le, and C. D. Lin, Phys. Rev. A **83**, 053409 (2011).
[65] S.-F. Zhao, C. Jin, R. R. Lucchese, A.-T. Le, and C. D. Lin, Phys. Rev. A **83**, 033409 (2011).
[66] R. R. Lucchese and V. McKoy, Phys. Rev. A **26**, 1406 (1982).
[67] C. Jin, A.-T. Le, S.-F. Zhao, R. R. Lucchese, and C. D. Lin, Phys. Rev. A **81**, 033421 (2010).
[68] X. Zhou, R. Lock, N. Wagner, W. Li, H. C. Kapteyn, and M. M. Murnane, Phys. Rev. Lett. **102**, 073902 (2009).
[69] A.-T. Le, R. R. Lucchese, and C. D. Lin, Phys. Rev. A **82**, 023814 (2010).
[70] M. Lein, R. D. Nalda, E. Heesel, N. Hay, E. Springate, R. Velotta, M. Castillejo, P. L. Knight, and J. P. Marangos, J. Mod. Opt. **52**, 465 (2005).
[71] M. B. Gaarde, J. L. Tate, and K. J. Schafer, J. Phys. B **41**, 132001 (2008).
[72] X. M. Tong, Z. X. Zhao, and C. D. Lin, Phys. Rev. A **66**, 033402 (2002).
[73] S.-F. Zhao, C. Jin, A.-T. Le, T. F. Jiang, and C. D. Lin, Phys. Rev. A **81**, 033423 (2010).
[74] C. Jin, H. J. Wörner, V. Tosa, A.-T. Le, J. B. Bertrand, R. R. Lucchese, P. B. Corkum, D. M. Villeneuve, and C. D. Lin, J. Phys. B **44**, 095601 (2011).
[75] C. Jin, S.-J. Wang, S.-F. Zhao, A.-T. Le, and C. D. Lin, Phys. Rev. A **102**, 013108 (2020).
[76] R. Torres, T. Siegel, L. Brugnera, I. Procino, J. G. Underwood, C. Altucci, R. Velotta, E. Springate, C. Froud, I. C. E. Turcu *et al.*, Opt. Express **18**, 3174 (2010).
[77] M. Negro, M. Devetta, D. Facciala, S. De Silvestri, C. Vozzi, and S. Stagira, Faraday Discuss. **171**, 133 (2014).
[78] L. E. Chipperfield, J. S. Robinson, J. W. G. Tisch, and J. P. Marangos, Phys. Rev. Lett. **102**, 063003 (2009).
[79] E. Balogh, B. Bódi, V. Tosa, E. Goulielmakis, K. Varjú, and P. Dombi, Phys. Rev. A **90**, 023855 (2014).
[80] C. Jin and C. D. Lin, Chin. Phys. B **25**, 094213 (2016).
[81] S.-F. Zhao, C. Jin, A.-T. Le, T. F. Jiang, and C. D. Lin, Phys. Rev. A **80**, 051402(R) (2009).
[82] I. Thomann, R. Lock, V. Sharma, E. Gagnon, S. T. Pratt, H. C. Kapteyn, M. M. Murnane, and W. Li, J. Phys. Chem. A **112**, 9382 (2008).
[83] M. Abu-samha and L. B. Madsen, Phys. Rev. A **80**, 023401 (2009).